

# Spatio-temporal irregularity in an excitable medium with shear flow

V. N. Biktashev[\*], I. V. Biktasheva[\*],

A. V. Holden, M. A. Tsyganov[†],

*Department of Physiology,*

J. Brindley and N. A. Hill,

*Department of Applied Mathematics,*

*University of Leeds, Leeds LS2 9JT, UK*

Submitted to PRL 1999/11/16; accepted to PRE 1999/04/02

## Abstract

We consider an excitable medium moving with relative shear, subjected to a localised disturbance which, in a stationary medium, would produce a pair of spiral waves. The spiral waves so created are distorted and then broken by the motion of the medium. Such breaks generate new spiral waves, and so a “chain reaction” of spiral wave births and deaths is observed. This leads to a complicated spatio-temporal pattern, the “frazzle gas” (term suggested in [5]), which eventually fills the whole medium. In this paper, we display and interpret the main features of the pattern.

PACS: 82.40.Bj, 47.70.Fw, 82.40.Ck, 87.10.+e,

**Introduction** Excitable medium models, in the form of partial differential equations of the reaction-diffusion type, have been used to account for nonlinear wave phenomena in many areas of biology, physical chemistry and physics [1]. An excitable system responds to a small subthreshold perturbation by a graded, decremental response, and to a suprathreshold perturbation by a large amplitude pulse or pulse train. This threshold property is characteristic of a cubic nonlinearity, as in the FitzHugh-Nagumo equations for an excitation process  $E$  and a recovery process  $g$ . In a spatially extended system, the suprathreshold response is a non-decremental travelling wave or a wave train. When such a cubic nonlinearity is included in a reaction-diffusion equation

$$\begin{aligned}\frac{\partial E}{\partial t} &= c_1 E(E - a)(1 - E) - g + D\nabla^2 E, \\ \frac{\partial g}{\partial t} &= \epsilon(c_2 E - g) + \delta D\nabla^2 g,\end{aligned}\tag{1}$$

in a two-dimensional medium, appropriate initial conditions can lead to a spiral wave. Such spiral waves (or scroll waves in three-dimensions) have been observed in many biological excitable media, and a spiral source acts to organise the surrounding medium.

When the excitable medium, such as a fluid or an elastic solid, is itself undergoing spatial strain, the otherwise stable spiral pattern is deformed and possibly broken. The effects of the motion of the medium on excitation-wave dynamics in the Belousov-Zhabotinsky system has been studied experimentally for thermoconvective motion in [2], and experimentally and theoretically for small deformations in [3].

We have shown that an arbitrarily small, linear shear flow can break repetitive wavetrains [4]. In a medium subject to a shear flow, the wavelength of the train changes with time. This change depends on the mutual orientation of the flow and wavetrain. In excitable media, there is a shortest possible wavelength, below which the waves cannot propagate. When the flow deforms the wavetrain so that wavelength is less than this critical value, the propagation is blocked. If the wavetrain and/or the flow is not strictly periodic, the blocking is localised and the waves that extend across a ‘blocked’ and ‘unblocked’ region break. The minimum time for the first wavebreak to occur has been estimated in [4] as

$$t_* \approx \alpha^{-1}(k_* - 1/k_*), \quad (2)$$

where  $\alpha$  is the shear (*i.e.* the gradient of the flow velocity), and  $k_*$  is the critical deformation, *i.e.* the ratio of the initial wavelength of the train and the minimum wavelength.

Here we consider the effects of simple shear flows on spiral wave behaviour in excitable media and show that spiral wave activity is broken down by *arbitrarily small shear flows* into spatio-temporal irregularity (an autowave turbulence, or “frazzle gas” similar to one described by Markus *et al.* [5]).

**The numerical model** For simplicity the numerical illustrations were performed using a FitzHugh-Nagumo system with cubic nonlinearity and added shear flow. We expect other excitable systems to display qualitatively similar behaviour. The equations considered were:

$$\begin{aligned} \frac{\partial E}{\partial t} &= c_1 E(E - a)(1 - E) - g + v(y) \frac{\partial E}{\partial x} + D \nabla^2 E, \\ \frac{\partial g}{\partial t} &= \epsilon(kE - g) + v(y) \frac{\partial g}{\partial x} + \delta D \nabla^2 g, \end{aligned} \quad (3)$$

with parameters  $c_1 = 10$ ,  $a = 0.02$ ,  $\epsilon = 0.1$ ,  $k = 5$ ,  $\delta = 1$  and  $D = 1$ . This system was solved using an explicit Euler scheme, with space step  $h_s = 0.5$  s.u. (space units) and time step  $h_t = 0.0025$  t.u. (time units), in a rectangular medium  $(x, y) \in [0, L] \times [-M/2, M/2]$ . The sizes  $L \times M$  were varied in different experiments. We used two flow velocity profiles, a linear profile

$$v(y) = \alpha y, \quad (4)$$

with no-flux boundary conditions at  $y = \pm M/2$ , and a sine profile

$$v(y) = v_{\max} \sin(2\pi y/M). \quad (5)$$

with periodic boundary conditions at  $y = \pm M/2$ . In all cases, we used periodic boundary conditions at  $x = 0, L$ . The properties of the stationary ( $\alpha = 0$ ) medium were as follows: the minimum wavelength of a periodic train  $\lambda_{\min} \approx 19.0$  s.u., the asymptotic wavelength of the spiral wave  $\lambda_{\text{s.w.}} \approx 41.0$  s.u., and the asymptotic velocity of the spiral wave  $c_{\text{s.w.}} = 1.80$  s.u./t.u.. The initial condition for this system was a short excitation wavelet, just wide enough to give birth to a pair of spiral waves (“horseshoe pattern”) as shown in Fig. 1(a).

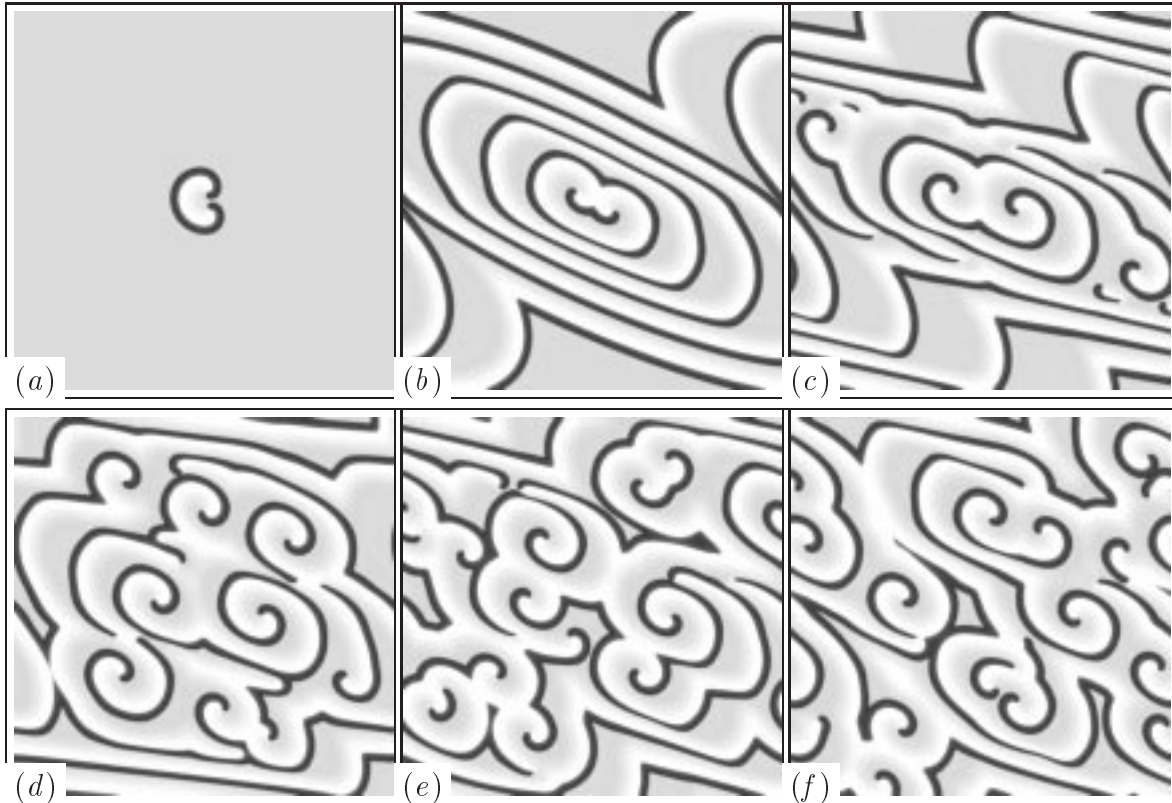


Figure 1: Development of a “frazzle gas” of spiral waves in linear shear flow (4). Shown are snapshots of  $E$  field at successive 100 t.u., in a  $400 \times 400$  s.u. medium, with a flow velocity gradient  $\alpha = 0.02$  t.u. $^{-1}$ .

**Development of the frazzle gas** The phenomenon of conduction blocking of periodic wavetrains has macroscopic consequences for the properties of large-scale two dimensional excitable media with shear flow. Since this conduction block is dependent on the orientation of the waves, it leads to breaking of the waves when there is a complicated autowave pattern. Moreover, in an excitable medium, each wavebreak typically leads to the generation of a new pair of spiral waves, which are sources of periodic wavetrains. This leads to a “chain reaction” of spiral wave births, as shown in Fig. 1.

Here a local finite initial perturbation has led to transition of the whole medium into a turbulence-like state, the “frazzle gas”. To characterise quantitatively the complexity of

the frazzle gas solution, we counted the number of the free ends, defined as intersections of the isolines  $E = 0.2$  and  $g = 0.48$ . Some typical dependencies of this number on time, for different values of the velocity gradient  $\alpha$ , are shown in Fig. 2. It appears that for any  $\alpha$ , a statistically steady value is reached after an initial period of development.

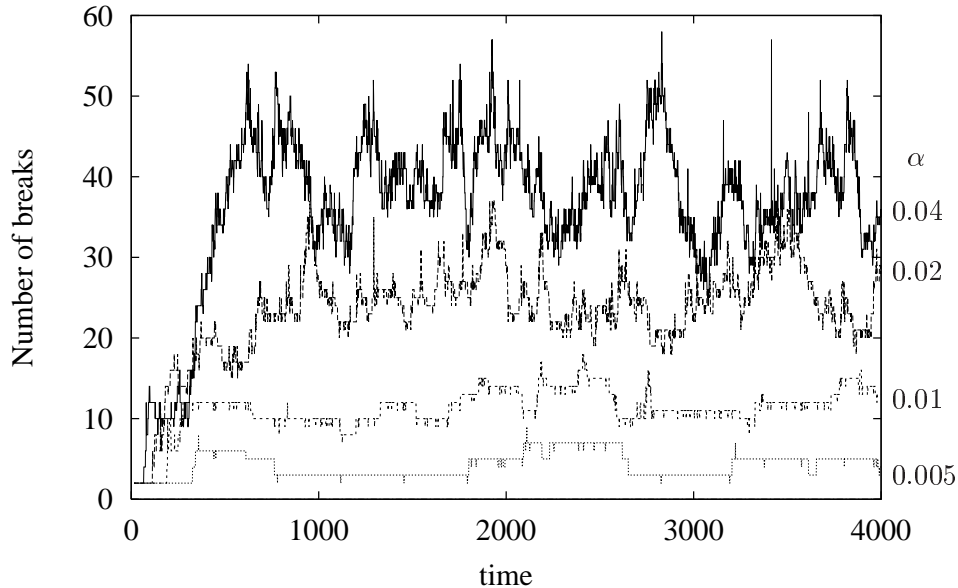


Figure 2: Number of free ends as function of time, in t.u., for different velocity gradients (values of  $\alpha$  shown in t.u. $^{-1}$ ), in a  $300 \times 300$  s.u. medium.

**Density of the frazzle gas** As can be seen in Fig. 1, the dynamics of the generation of new wavebreaks in this particular experimental setup is determined, in the first instance, by two different processes: the growth of the “horseshoe” pattern, due to the revolution of the spiral waves, and the deformation of that pattern. Subsequently, the development of secondary breaks further increases the density of the free ends, until the pattern reaches a state of statistical equilibrium, when the average number of the new free ends is balanced by the average rate of their annihilation, which happens if two opposite free ends come too close to each other. The resulting pattern and fluctuations in the number of free ends depends on the value of the velocity gradient, as illustrated in Fig. 3.

The simple criterion for the wave break introduced in [4] can be used for a rough analytical estimate of the equilibrium density of spiral waves. First, let us estimate the typical distance between the spiral waves as being of the same order of magnitude as the distance from the spiral center to the point at which the first break in a spiral wave occurs. This is made up of a minimum distance, of the order of the spiral core, or spiral wavelength  $\lambda_{s.w.}$ , plus the distance travelled by the spiral wave in the time before the breakup, which is  $t_* \approx \alpha^{-1}(k_* - 1/k_*) \propto \alpha^{-1}$ , since the critical deformation  $k_* = \lambda_{\min}/\lambda_{s.w.} \approx 2.16$ . The

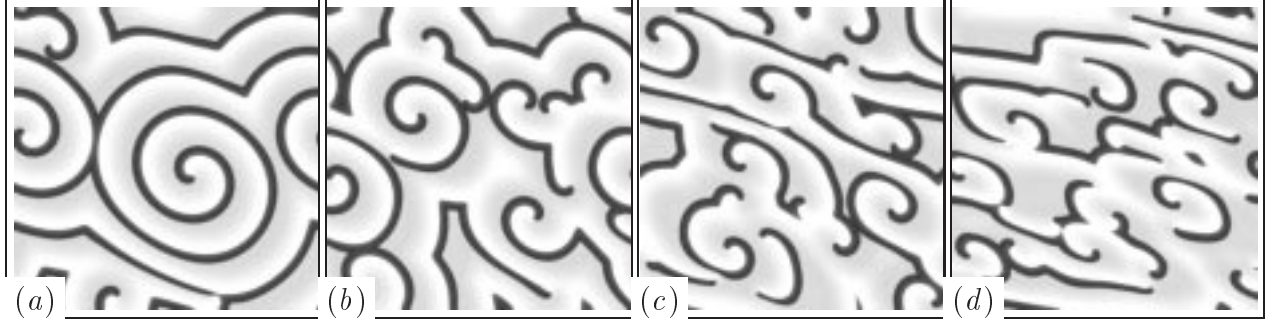


Figure 3: Structure of the dynamically equilibrated “frazzle gas” of spiral waves (snapshots of the  $E$  field) at different velocity gradients: (a)  $0.005 \text{ t.u.}^{-1}$ , (b)  $0.01 \text{ t.u.}^{-1}$ , (c)  $0.02 \text{ t.u.}^{-1}$  and (d)  $0.04 \text{ t.u.}^{-1}$ . Size of the medium  $300 \times 300 \text{ s.u.}$

typical distance between the spiral waves in the frazzle gas can thus be expected to be

$$l_{\text{s.w.}} = \beta \lambda_{\text{s.w.}} + \gamma c_{\text{s.w.}} \alpha^{-1}. \quad (6)$$

where  $\beta$  and  $\gamma$  are some dimensionless coefficients of the order of 1. The density of the spiral waves is then estimated by

$$\rho = l_{\text{s.w.}}^{-2} = \alpha^2 / (K_1 + K_0 \alpha)^2, \quad (7)$$

where

$$K_0 = \beta \lambda_{\text{s.w.}}, \quad K_1 = \gamma c_{\text{s.w.}}. \quad (8)$$

Fig. 4 shows the dependence  $\rho(\alpha)$  found in numerical experiments, and the best fit to (7). This best fit is achieved with  $K_0 \approx 36$  and  $K_1 \approx 0.46$ , which means  $\beta \approx 1.9$  and  $\gamma \approx 0.26$ . Thus, the simple argument presented above correctly predicts the qualitative dependence of  $\rho$  on  $\alpha$ , for a reasonable choice of the dimensionless coefficients. Recall that the estimates of [4] also were only valid to within an order of magnitude.

**Frazzle gas in an inhomogeneous flow** The linear shear is a highly simplified case. To check the robustness of the features of the frazzle gas of spirals, we studied its behaviour in a more complicated flow, the sine shear flow (5). The results are illustrated in Fig. 5.

The sine shear profile (see panel  $t = 6$  of Fig. 5) provides two regions with high velocity gradient, clockwise in the middle ( $y \approx 0$ ) and counterclockwise around the upper and lower boundary ( $y \approx \pm M/2$ , recall that the boundary conditions are periodic), and two regions with lower velocity gradient, around  $y \approx M/4$  and  $y \approx -M/4$ . The horseshoe pattern is initiated in the region with high shear, and is first ( $t = 12$ ) and then displays wavebreaks ( $t = 24$ ). In turn, the free ends curl into new spirals, which lead to secondary breaks ( $t = 48$ ) and subsequently to the frazzle gas of spirals ( $t = 96$ ). At  $t = 96$ , one can see that the frazzle gas is localised in the high-shear region, but some of the spirals are driven away from that region (notice the two spirals at  $x \approx 3L/4$ ,  $y \approx M/4$ , and at  $x \approx L/4$ ,  $y \approx -M/4$ ), and that the nearly-plane wavetrains are compressed in the other high-shear

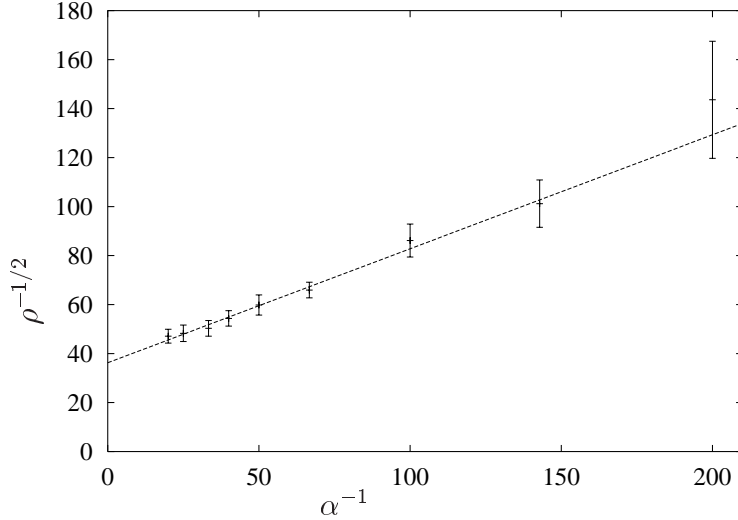


Figure 4: Time-average density of free ends,  $\rho$ , measured in  $\text{s.u.}^{-2}$ , for established “frazzle gas” state, as function of the velocity gradient,  $\alpha$ , measured in  $\text{t.u.}^{-1}$ , in coordinates  $\rho^{-1/2}$  vs  $\alpha^{-1}$ . Points with errorbars show values obtained from simulation, the lines show the best fit to the theoretical dependence (7).

region (see near the upper and lower boundaries). This subsequently leads to the generation of the frazzle gas in the other high-shear region ( $t = 192$ ), which with time relaxes to a dynamic macroscopic equilibrium state ( $t = 384$ ) This then remains statistically constant — or at least does not qualitatively change over the following time interval ( $t = 768$ ).

The structure of the frazzle gas is inhomogeneous, and may seem counterintuitive. The free ends are seen in both high- and low-shear regions. In high-shear regions, one can see well developed spiral waves, while in low-shear regions, where in the homogeneous case one would expect even better developed spirals (see Fig. 3(a)), there are no spirals at all, but only dislocations in quasi-plane wave trains.

This paradox is easily explained. The presence of a shear flow breaks the spatial reflection symmetry of the reaction-diffusion system. As a result, the angular velocity of a spiral wave in the shear flow now depends on the direction of rotation. The general perturbation theory [6] predicts only that the angular velocity is

$$\omega = \omega_0 + \chi m \alpha + O(\alpha^2), \quad (9)$$

where  $\omega_0$  is the angular velocity in a quiescent medium,  $m$  is direction of rotation, say  $m = 1$  for clockwise rotating spirals and  $m = -1$  for counterclockwise, and coefficient  $\chi$  depends on the particular model. In our model, the spirals rotating against the shear (counter-rotating spirals) rotate faster.

Furthermore, it is well known that, in an autowave medium, faster sources entrain slower sources, and if the slower source is a spiral wave, this causes its so-called “induced drift” [7, 8, 9]. As a result, in the high-shear regions, co-rotating spiral waves are entrained

$y$ range	$[0, M/8] \cup [7M/8, M]$	$[M/8, 3M/8]$	$[3M/8, 5M/8]$	$[5M/8, 7M/8]$
shear	high c.c.w.	small	high c.w.	small
$t = 384$	11/2 (c.w./c.c.w)	10/12	3/13	7/7
$t = 768$	11/3	10/10	4/12	6/5

Table 1: Structure of the frazzle gas in different regions. The ratios show number of c.w. free ends/number of c.c.w free ends in the region.

by counter-rotating spirals and driven away to the low-shear regions. The spirals in the low-shear regions do not develop since the spiral rotation frequency there is approximately  $\omega_0$ , which is lower than that in the high-shear regions where it is  $\omega_0 + |\chi\alpha_{\max}|$ , so the free ends remain dislocations and cannot develop into spiral waves.

These processes lead to the following structure (see Table 1). The high-shear regions are populated mainly (but not exclusively) by counter-rotating spirals, *i.e.* counterclockwise rotating in the middle region and clockwise rotating in the top/bottom region. However, some corotating spirals are also present, since the free ends are born in pairs, and it takes time to entrain a spiral wave. At the same time the low-shear regions show quasi-plane wave trains with dislocations, which are former spiral waves expelled from the high-shear regions.

**Discussion** In this paper, we have described the process of generation and main properties of a “frazzle gas” of spiral waves produced by shear flows in the medium. Such a frazzle gas occurs in a sufficiently large excitable medium when shear flow breaks a repetitive wavetrain. The conditions for the generation of the first wavebreaks were described earlier [4] and the first break requires a space and time to develop (the weaker the shear, the larger the space and time required), whereafter new wavebreaks are generated via a chain reaction, until a dynamical equilibrium is reached where the average number of newly generated wavebreaks equals the average number of annihilated wavebreaks.

The average density of wavebreaks as a function of flow velocity gradient is described by a simple semi-empirical “Michaelis-Menten” formula; understanding the key mechanisms of the dynamic equilibrium allowed us to relate, to within the order of magnitude, the constants in that formula to principal parameters of the medium.

An inhomogeneously sheared flow makes the rate of generation of new wavebreaks space-dependent, which naturally leads to inhomogeneous distribution of the wavebreak. In addition, it introduces qualitatively new features, especially if the shear changes sign: the flow sorts the wavebreaks by their chirality. The mechanism for this sorting is related to parity violation by the shear, which leads to a difference in frequency between oppositely rotating spiral waves and to induced drift of the slower rotating waves.

The mechanism and properties of this “frazzle gas” makes it different from other examples. In particular, the example in [5] is clearly different since it occurs in a stationary medium. The experimental example [2] is more similar, since it is also about interaction of convection and excitation. However, the convection there was quite complicated, con-

sisting of Bénard convection cells, of size comparable to the wavelength of the spiral. It was therefore not clear whether the complexity of the resulting pattern should have been attributed to the presence of convective motion or to its complexity. The present study shows that the complexity of the flow is not necessary, as the irregular activity occurs even in a perfectly homogeneous linear shear flow.

**Acknowledgement** This work has been supported by grants from Wellcome Trust 045192, EPSRC GR/L 73364 and INTAS-96-2033.

## References

- [\*] On leave from Institute for Mathematical Problems in Biology, Pushchino, Moscow region, 142292, Russia
- [†] Also with Institute for Theoretical and Experimental Biophysics, Pushchino, Moscow region, 142292, Russia
- [1] *Nonlinear Wave Processes in Excitable Media*, edited by A. V. Holden, M. Markus, and H. G. Othmer (Plenum, New York, 1991).
- [2] K. I. Agladze, V. I. Krinsky and A. M. Pertsov, *Nature* **308**, 834 (1984)
- [3] A. P. Munuzuri *et al.*, *Phys. Rev. E* **50**, R 667 (1994).
- [4] V. N. Biktashev *et al.*, *Phys. Rev. Lett.* **81**, 2815 (1998).
- [5] M. Markus, G. Kloss, and I. Kusch, *Nature* **371**, 402 (1994).
- [6] V. N. Biktashev and A. V. Holden, *Chaos, Solitons and Fractals* **5**, 575 (1995).
- [7] E. A. Ermakova, V. I. Krinsky, A. V. Panfilov, and A. M. Pertsov, *Biofizika* **31**, 318 (1980).
- [8] V. I. Krinsky and K. I. Agladze, *Physica D* **8**, 50 (1983).
- [9] V. N. Biktashev, in *Computational Biology of the Heart*, edited by A. V. Panfilov and A. V. Holden (Wiley, Chichester, 1997), pp. 138–170.



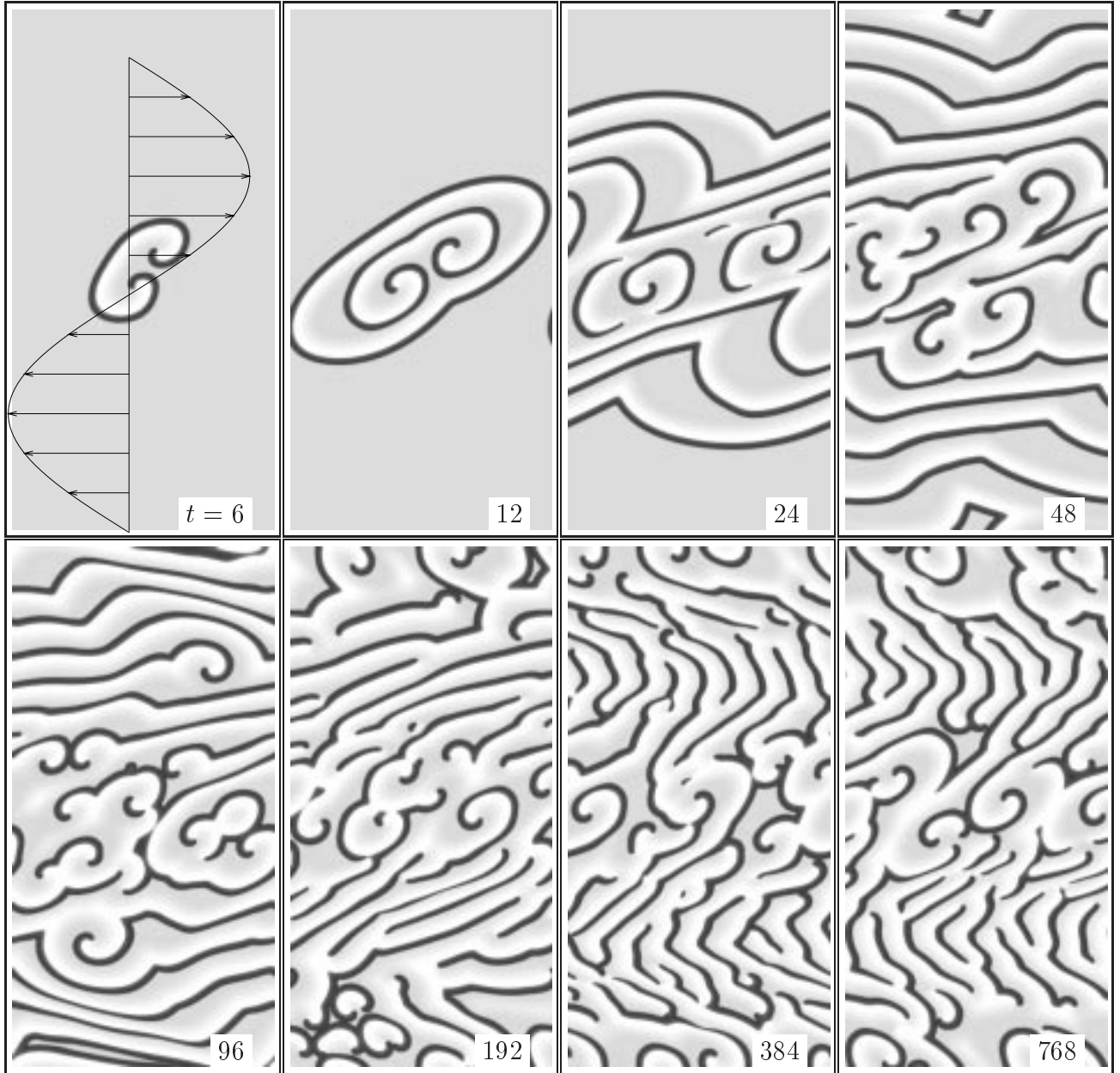


Figure 5: Development of a “frazzle gas” of spiral waves in a sine-shear flow (5). Shown are snapshots of  $E$  in a  $300 \times 600$  s.u. with maximal flow velocity  $v_{\max} = 1.5 \text{ s.u.} \cdot \text{t.u.}^{-1}$  at time moments (shown on each panel, measured in t.u., ) chosen in geometric progression.  $h_x = 1.0$ ,  $h_t = 0.01$ .